This article has been accepted for publication in a future issue of this journal, but has not been fully edited. Content may change prior to final publication. Citation information: DOI 10.1109/JSEN.2017.2765745, IEEE Sensors Journal

Screen-printed curvature sensors for soft robots

Anastasia Koivikko, Ehsan Sadeghian Raei, Mahmoud Mosallaei, Matti Mäntysalo, *Member IEEE*, and Veikko Sariola, *Member IEEE*

***Abstract*— Castable elastomers have been used to fabricate soft robotic devices and it has been shown that the technique scales well from prototyping to mass manufacturing. However, similarly scalable techniques for integrating strain or curvature sensors into such devices are still lacking. In this paper, we show that screen-printed silver conductors serve well as curvature sensors for soft robotic devices. The sensors are produced onto elastomer substrates in a single printing step and integrated into soft pneumatic actuators. We characterized the resistance-curvature relationship of the sensors, which allows the curvature of the actuators to be estimated from the sensor measurements. Hysteresis was observed, which does limit the absolute accuracy of the sensors. However, temperature characterizations showed that the sensor measurements are not significantly affected by temperature fluctuations during normal operation. Dynamic experiments showed that the bandwidth of the sensors is larger than the bandwidth of the actuators. We experimentally validated that these sensors can be used to detect whether the motion of an actuator has been blocked, clearing the way towards simple-to-fabricate soft robots that react to their surroundings. Finally, we demonstrate a three-fingered soft robotic gripper with integrated sensors. We conclude that screen-printing is a promising way to integrate curvature sensors into soft robots.**

***Index Terms*—Mechanical Sensors, Flexible printed circuit, Soft robotics, Strain measurement**

I. Introduction

Soft robots [1]–[4] made of easily deformable materials are a recent innovation with promising applications in manipulators/grippers [2], [5]–[7], mobile robots [8]–[10], exoskeletons/rehabilitation [11] and monitoring human motion [12]. Soft actuators have been made by embedding small fluidic channels in an elastomer, and then inflating them by gas [2], [13], [14] or liquid [15]. The quick, monolithic fabrication technique of casting elastomers into 3D printed molds has enabled the rapid prototyping of different soft robot designs [2], [10], [16], and this technique scales well for mass manufacturing. However, in their simplest form, the fluidic actuators do not include any strain or curvature sensors. Such sensors would enable closed-loop position control or the ability to detect whether an obstacle is blocking the motions of the robot.

The first approach to integrating sensors into soft robots was to embed commercially available bending sensors [17], [18] or custom-designed sensor modules [19] into the casting/assembly. However, this approach is not ideal as the sensor design cannot be adapted quickly to new robot designs. The second approach was to fabricate flexible/stretchable sensors [20]–[23] as needed. Flexible or stretchable strain sensors based on carbon nanotubes [24], carbon black particles [25], liquid metals [12], [26], and silver nanowires [27], [28] have all been proposed. In particular, carbon nanotubes [29], hydrogels [30], liquid metals [31] and optical sensing [32], [33] have been utilised for curvature sensing in soft fluidic actuators. However, many of these examples involve multistep fabrication or materials which are difficult to handle, so they are not suitable for mass manufacturing. There is still a clear need for a simple, low-cost and scalable method for manufacturing sensors for soft robots.

Printed electronics as an additive manufacturing method is a good candidate to fulfill these needs. Functional materials have been printed to fabricate flexible circuits [34], temperature sensors [35] and electrodes [36]. Screen-printing, in particular, is the most common printing method used in electronics. Screen-printing is one of the oldest printing technologies in existence, originating in China over a thousand years ago. Today, screen-printing is applied not only in electronics, but also in textiles, signs, product labels and many other products. Consequently, screens, inks and automated printing machines are widely available.

Recently, our coauthors have shown that screen-printing with conductive inks can be used to produce stretchable conductors directly onto elastomer substrates [37]. Here we show that these conductors, printed in a single step, can serve as resistive curvature sensors for soft robots. These sensors yield information about the true curvature of a soft robotic actuator within the limits of the hysteresis and the creep of the sensor. By creep, we mean slow change observed in the sensor output, even when the actuator is not moving. The main advantages of these sensors are that they: a) can be fabricated in a matter of hours; b) require only a little extra effort in the fabrication of the actuators; and c) are based on widely available equipment and materials.

Submitted on June 11, 2017. Revised on September 3, 2017. An earlier version of this paper was submitted to the IEEE Sensors 2017 Conference. This work was supported by the Academy of Finland, projects #299087, #306999, #288945 and #294119.

A. Koivikko, E. Sadeghian Raei, and V. Sariola are with the BioMediTech institute and Faculty of Biomedical Sciences and Engineering, Tampere University of Technology, Tampere, 33720 Finland (email: veikko.sariola@tut.fi)

M. Mosallaei and M. Mäntysalo are with the Laboratory of Electronics and Communications Engineering, Tampere University of Technology, Tampere, 33720 Finland (e-mail: matti.mantysalo@tut.fi)

This work is licensed under a Creative Commons Attribution 3.0 License. For more information, see http://creativecommons.org/licenses/by/3.0/.

This article has been accepted for publication in a future issue of this journal, but has not been fully edited. Content may change prior to final publication. Citation information: DOI 10.1109/JSEN.2017.2765745, IEEE Sensors Journal

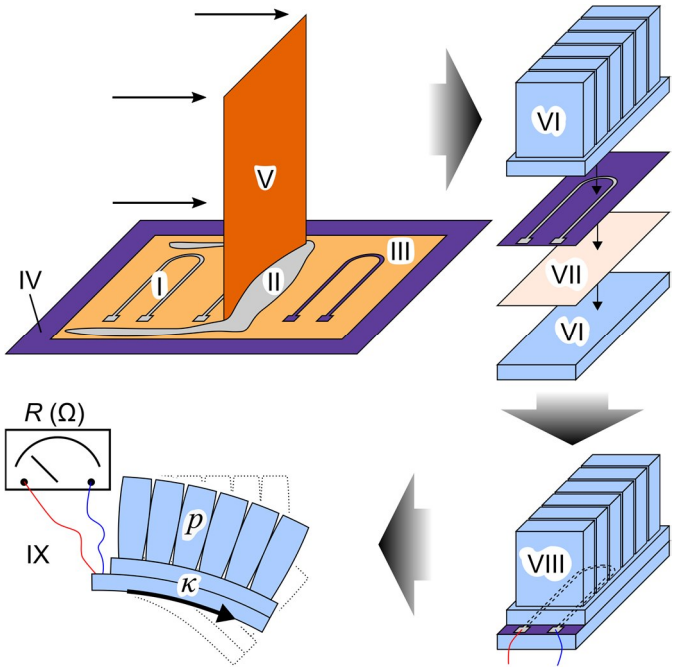

Fig. 1. The concept of soft actuators with sensors. The sensors (I) are screen-printed by applying a resistive silver or carbon ink (II) on a screen (III) lying on top of a polyurethane elastomer substrate (IV). The ink is spread by a squeegee (V). By assembling a stack of silicone components (VI), a fiberglass strain-limiting layer (VII) and a sensor, a smart pneumatic actuator (VIII) is produced. The actuator is pressurized with the pressure p. The measuring resistance R (IX) gives the curvature κ of the actuator.

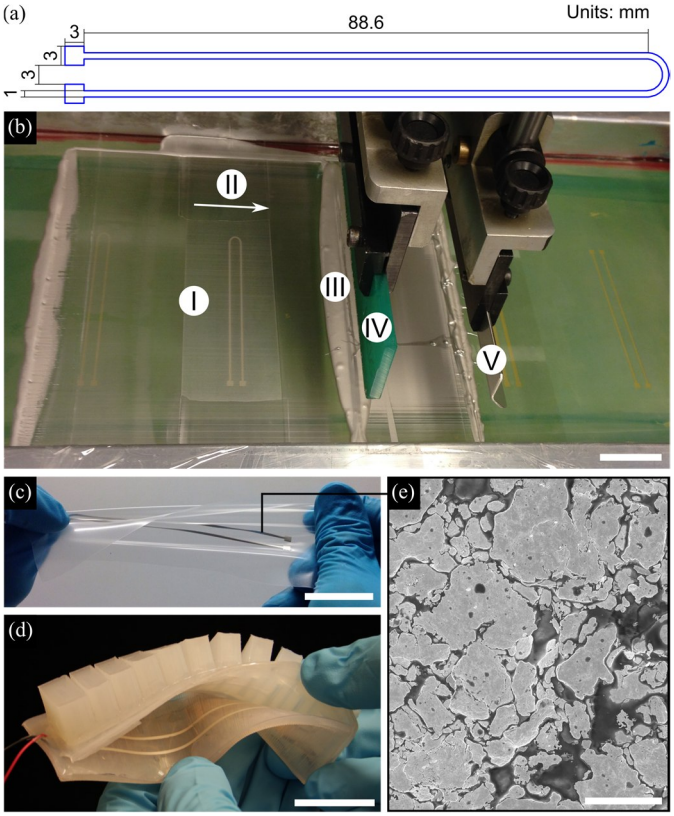

Fig. 2. Fabrication results. (a) Print design of the sensors. Units: mm. (b) Photograph of the screen-printing process. I: Mesh/screen. II: Print direction. III: Silver ink. IV: Rubber squeegee. V: Metal squeegee. (c) Photograph of the sensor. (d) Photograph of the actuator. Scale bars in all photographs: 3 cm. (e) Scanning electron micrograph of the screen-printed silver sensors. The light areas are silver flakes and the darker background is polymer. Scale bar: 10 µm.

II. Materials and Methods

A. Overview of the fabrication method

The fabrication method is illustrated in Fig. 1. Conductive ink was added onto a screen lying on a thermoplastic polyurethane elastomer sheet. The ink is transferred to the substrate through a mesh, except in the areas covered by a stencil.

In a single step, we fabricate a shape with two pads and a long, conductive path (Fig. 2a). We used a silver flake-based ink for the sensors. A photograph of the screen-printing process is shown in Fig. 2b. After printing, the sensors are wired, cut and integrated into the pneumatic actuators. The actuator consists of two parts: an upper part with pneumatic chambers and a base with a strain-limiting layer (fiberglass). Upon pressurizing, the pneumatic chambers expand, resulting in the bending of the actuator. The sensors are stacked on top of the strain-limiting layer before the assembly of the actuator. Resistance measurement can be used to estimate the curvature κ of the actuator. Photographs of the fabricated silver sensors and actuators are shown in Fig. 2 c-d. A scanning electron micrograph (Fig. 2e) shows the flaked structure of the screen-printed silver. The stretchability of these conductors comes from this microstructure [37].

B. Fabrication of the curvature sensors

The sensors were fabricated on thermoplastic polyurethane substrate (Epurex Platilon / U4201), which is a stretchable, abrasion resistant, chemically inert, 50 µm thick, transparent sheet. Most of the results in this paper were done using silver ink (ECM / CI-1036), but we also tested carbon ink (ECM / CI-2051) for comparison. The silver ink had a quoted sheet resistance of < 10 mΩ sq^{-1} at 25.4 µm and a curing temperature of 120ºC for 10 minutes, which is lower than the softening range of the elastomer. The carbon ink had a quoted sheet resistance of < 40 Ω sq^{-1} at 25.4 µm. The screens (Finnseri Oy) had a mesh count of 79 threads cm^{-1} and a mesh opening of 69 μm^{-1}.

The screen-printing starts by slightly stretching the substrate and attaching it to an aluminum plate. The substrates are then cleaned with isopropyl alcohol. The printing is done in two continuous printing cycles by a semi-automatic screen-printing machine (TIC / SCF-300). The process is completed with an oven annealing (silver ink: 30 min at 125 °C, and carbon: 10 min at 90 °C). The annealing temperature and time were increased for the silver due to the heat absorption of the aluminum carriers [35]. The sheet resistances of the silver and carbon traces (measured after the annealing) are approximately 45 mΩ sq^{-1} and 300 Ω sq^{-1}, respectively. Finally, wires are attached to the pads of the conductive print using silver paint (MG Chemicals / 8331-14G).

C. Fabrication of the soft pneumatic actuators

The pneumatic actuator design is from Mosadegh *et al.* [14] and detailed drawings can be found in the Soft Robotics Toolkit

This work is licensed under a Creative Commons Attribution 3.0 License. For more information, see http://creativecommons.org/licenses/by/3.0/.

This article has been accepted for publication in a future issue of this journal, but has not been fully edited. Content may change prior to final publication. Citation information: DOI 10.1109/JSEN.2017.2765745, IEEE Sensors Journal

(http://softroboticstoolkit.com/) [16]. We cast silicone (Smooth-On / Dragon skin 30. Shore A hardness: 30) into 3D-printed plastic molds. The actuator consists of an upper part, with the pneumatic chambers, and a lower part, the base. The base is a stack of several layers: Dragon Skin 30, a fiberglass strain limiting layer, a sensor on polyurethane facing away from the fiberglass, and another layer of Dragon Skin 30. We bonded all the parts using a silicone adhesive.

In our initial trials, when we placed the sensor on the outer bottom wall of the actuator, the sensors delaminated easily. In our final design, the sensors were placed inside the actuator to avoid this delamination. The last layer of Dragon Skin 30 on the sensors prevents slipping and delamination of the sensors while the actuators are moving.

D. *Resistance measurements*

We measured the resistance R of the sensors using a digital multimeter (National Instruments / USB-4065). Multichannel strain measurements were made using a strain/bridge input module (National Instruments / NI-9237). For the bridge measurements, 100 Ω or 102 Ω resistors were added in series with the sensors, while the quarter-bridge was made into a half-bridge with 120 Ω resistors.

E. *Pressure control*

The fluidic control board was based on the instructions from the Soft Robotics Toolkit (http://softroboticstoolkit.com/) [16]. Briefly, solenoid valves were driven by an Arduino microcontroller using pulse-width modulation at 56 Hz. The pressure p was controlled by changing the duty cycle of the valves. Pressure sensors measured the pressure p at the control board. Supply pressure was from a regulator at ~ 2 bar.

F. *Curvature measurements*

The actuator was mounted on an aluminum frame from the air inlet side (Supplementary Fig. 1). A computer-controlled digital camera took photographs. The photographs were saved along with the pressure and resistance data. The images were analyzed by a custom-designed Matlab script, which used an optimization algorithm to find a circular arc that best fit the pixels on the bottom edge of the actuator. The inverse of the arc radius is taken as a measure of the curvature κ. Note that the soft bending actuators do not have constant curvature κ, but it is still a reasonable estimate [38].

G. *Temperature measurements*

We used K- and J-type thermocouples to monitor the temperature of the actuator during the experiments.

III. Results and Discussion

A. *Resistance – curvature relationship of the silver sensors*

To characterize the silver sensors, we measured the resistance R and curvature κ while repeatedly cycling the pressure p of the actuator (30 cycles). Each cycle was slow (~ 5 min) to avoid dynamic effects from the viscoelasticity of the elastomers. The results of the measurements are shown in Fig. 3. In the initial state, $R = 15.8\ \Omega$, $p = 12$ kPa, and $\kappa = 7\ \mathrm{m}^{-1}$. At their peak, $\Delta R = 1.7\ \Omega$, $\Delta p = 47$ kPa and $\Delta\kappa = 21\ \mathrm{m}^{-1}$. The sensitivity was $0.075\ \Omega/m^{-1}$.

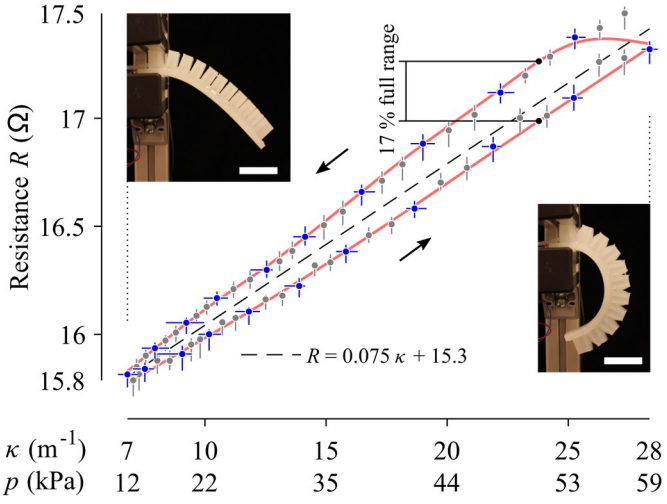

Fig. 3. Resistance R versus curvature κ and pressure p for the silver sensor. Curvature κ was estimated from photographs (insets). The data points are medians of 150 resistance measurements and 30 curvature measurements (blue points). The curvature κ had to be linearly interpolated between frames (gray data points). The error bars show interquartile range. The cycle was repeated 30 times. Scale bars in photographs: 3 cm.

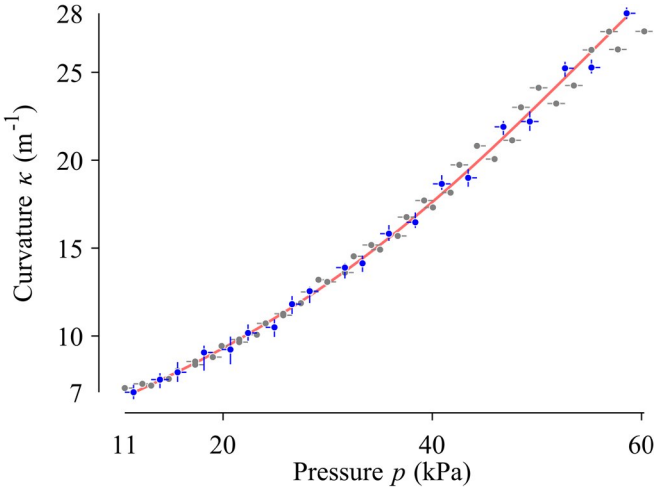

Fig. 4. Pressure-curvature relationship for the actuator used in Fig. 3. The return curve points are slightly above the fitted curve, but the effect is much smaller than in Fig. 3.

The relationship between resistance R and curvature κ is linear and hysteretic, with a maximum hysteresis of 17 % (Fig. 3). The relationship between pressure p and curvature κ is non-linear and without hysteresis (Fig. 4). This data is consistent with the previous reports of the hysteretic behavior of conductive inks [39]. However, even a linear resistance-curvature model has an R^2-statistic of 0.92. We conclude that the silver sensor can yield useful proprioceptive information from the actuator, limited by the hysteresis of the sensor material.

Note that the sensor is ~ 90 mm long, while the whole actuator is ~ 110 mm long. Each small segment of the sensor is responsive to local strains and thus to local curvatures of the actuator, but when we measure the total resistance of the sensor,

This work is licensed under a Creative Commons Attribution 3.0 License. For more information, see http://creativecommons.org/licenses/by/3.0/.

This article has been accepted for publication in a future issue of this journal, but has not been fully edited. Content may change prior to final publication. Citation information: DOI 10.1109/JSEN.2017.2765745, IEEE Sensors Journal

we are measuring the average curvature κ of the actuator, except in the small area at the tip not covered by the sensor. In practice, the local curvatures do not deviate much from the average curvature κ for these types of actuators [38].

B. Temperature – resistance relationship for the silver sensors

The data in Fig. 3 does not rule out that the hysteresis is caused by temperature fluctuations within each cycle. To rule out this possibility, we measured the temperature coefficient of resistance and the normal temperature fluctuations during the experiments. We placed the actuator flat on a hot plate and measured the resistance R as a function of the temperature. The thermocouple was inserted into the pneumatic chamber inside the actuator. The resistance R was recorded at the moment when the temperature was first reached. The results of these measurements are shown in Fig. 5. The temperature coefficient of the resistance is $(dR/dT)/R|_{T=20°C} \approx 0.01\ °C^{-1}$, which is slightly higher than the temperature coefficient of pure silver: $0.0038\ °C^{-1}$.

To see if this could contribute to the hysteresis in our cycling experiments, we measured the temperature fluctuations of the air entering or leaving the actuator. The air temperature was taken from the air entering / exiting the actuator, right next to the inlet. The results (Fig. 6) show that during the first cycle, the air heated up from 25.0 °C to 25.7 °C, but after the first few cycles, the temperature fluctuations are within $\Delta T \approx 0.3$ °C. These fluctuations are caused by our pressure controller, and the estimated contribution to resistance change is $(dR/dT)\Delta T \approx 0.04\ \Omega$. Thus, we conclude that the air temperature fluctuations cannot be the dominant effect to explain the hysteresis in Fig. 3.

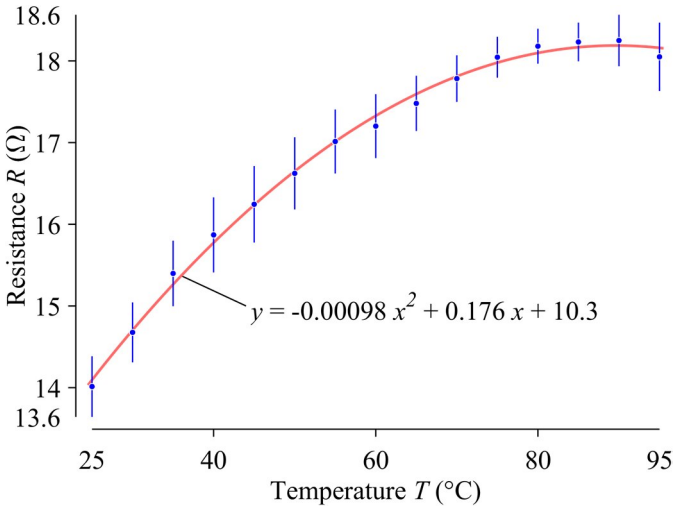

Fig. 5. Resistance R of a silver sensor as a function of the temperature T. Data points are means of six measurements, error bars show standard error.

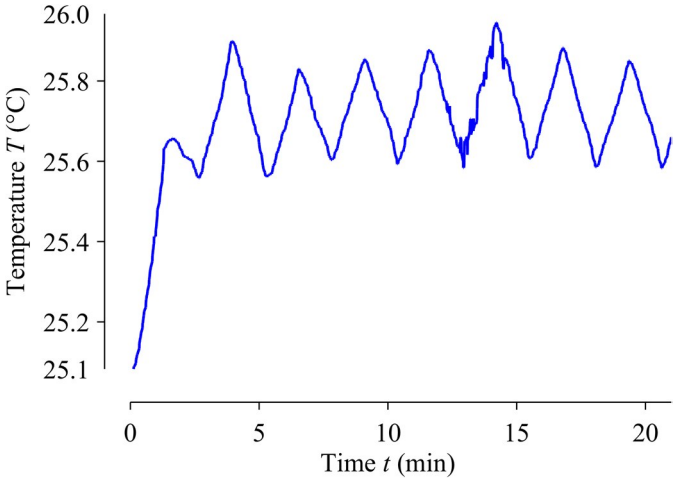

Fig. 6. Temperature fluctuations during the cycling experiment in Fig. 3.

C. Linear strain estimates

To estimate the linear strain ε for our silver sensors, our first approach was to use the ideal bending relationship

$$\Delta\varepsilon = d\Delta\kappa, \tag{1}$$

where d is the distance from the neutral plane. Assuming that the neutral plane is half-way through the fiberglass, the stack between the sensor and neutral plane is: fiberglass ($d = 125\ \mu m$, half of the nominal thickness), silicone adhesive (we take $d = 500\ \mu m$, but this is difficult to measure and varies from one sample to another) and polyurethane ($d = 50\mu m$, nominal), the total distance from the neutral plane is $d = 675\ \mu m$. Thus, using (1), we estimate $\Delta\varepsilon \approx 675\mu m \cdot 21 m^{-1} \approx 1\ \%$. Our second approach was to use ΔR and the previously reported [37] small-strain gauge factor of $GF \approx 5.759$ and the relationship

$$\Delta\varepsilon = \frac{\Delta R}{R \cdot GF}, \tag{2}$$

to estimate $\Delta\varepsilon \approx 2\ \%$. Because of the difficulties of measuring the thickness of the soft sensor stack and the distance from the neutral plane d, we consider the resistance-based estimate of 2% strains to be more trustworthy.

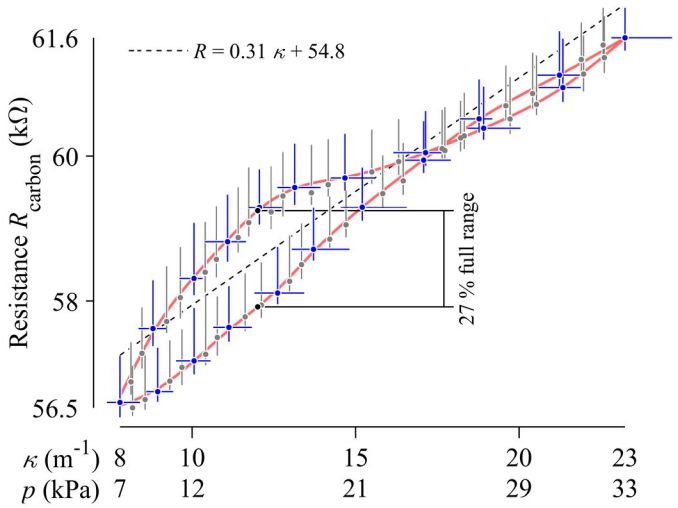

Fig. 7. Resistance R_{carbon} versus curvature κ and pressure p for the carbon sensor. Data points are medians of 150 resistance measurements and 30 curvature measurements (blue points). The curvature was interpolated for the gray data points. The error bars show interquartile range.

This work is licensed under a Creative Commons Attribution 3.0 License. For more information, see http://creativecommons.org/licenses/by/3.0/.

This article has been accepted for publication in a future issue of this journal, but has not been fully edited. Content may change prior to final publication. Citation information: DOI 10.1109/JSEN.2017.2765745, IEEE Sensors Journal

D. Carbon sensors

To show that our approach is not limited to silver-based inks, we also tested printing the sensors using carbon-based inks. The resistance-curvature characterization for the actuator with a carbon sensor is shown in Fig. 7. Due to the specific resistance of the ink being higher, the absolute resistances are also higher; in a neutral state, the resistance $R_{\text{carbon}} = 56.5\ k\Omega$. The sensitivity of the carbon sensor was $0.31\ \text{k}\Omega/\text{m}^{-1}$, and the maximum hysteresis 27 %. Compared to the silver sensors, there is more non-linearity and creep in the carbon sensors, which is why we focused on the silver sensors in our studies. Nevertheless, a linear resistance-curvature model still has a R^2-statistic of 0.64, supporting our claim that carbon sensors can also be used to estimate the bending of the actuator.

E. Decoupling pressure contribution from the curvature measurement

We then checked whether the pressure changes make a direct contribution to the silver sensor measurements. We measured the curvature κ, resistance R and pressure p in four different states (Fig. 8) , where the actuator was bent or prevented from bending by an external force (a hand) in addition to being driven by internal pressure. The resistance measurement is closer to the curvature measurement, but also shows some response to the pressure changes. The underlying reason for the pressure response is that the sensor responds to strains, but during pressurization of the actuator, not all strains are just from ideal bending. Simple linear decoupling found using the method of least-squares

$$\kappa_{\text{estimate}} = \alpha R + \beta p + \gamma, \qquad (3)$$

where $\alpha = 17.1\ \text{m}^{-1}\Omega^{-1}$, $\beta = -0.230\ \text{m}^{-1}\text{kPa}^{-1}$ and $\gamma = -254\ \text{m}^{-1}$ yielded the estimate shown in Fig. 8. Thus, approximately $\frac{\Delta\kappa}{\alpha\Delta R} \approx 70$ % of the sensor signal comes from the curvature changes alone. Furthermore, comparing κ_{estimate} to the pressure curve allows the detection of whether the actuator has been blocked or is being forced. We conclude that the sensor is mainly a curvature sensor and an external pressure measurement can be used to decouple the curvature estimate.

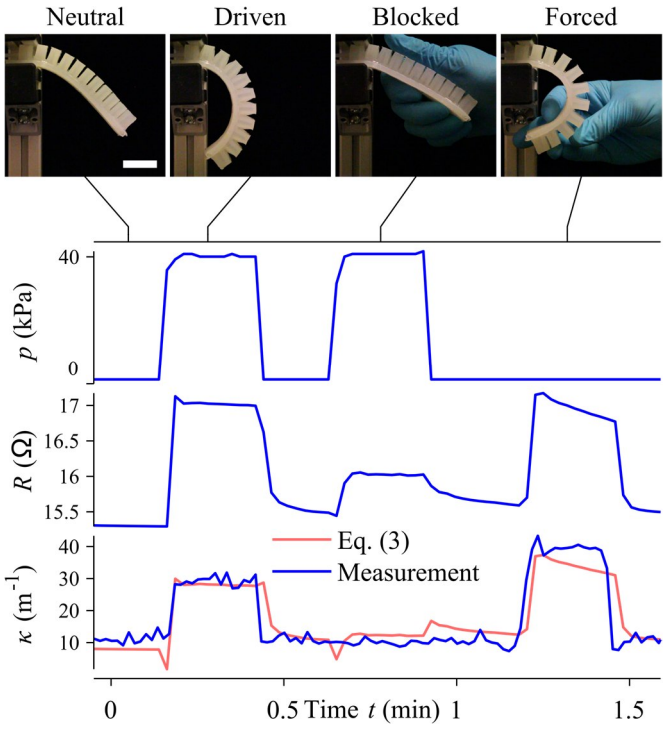

Fig. 8. Pressure p, resistance R and curvature κ recordings from the external blocking experiment. Snapshots are from a video. Scale bar: 3 cm.

F. Dynamic response of the actuator and the sensor

To study the dynamics of the system, we performed step experiments by fully opening or closing the valve, with the supply pressure adjusted to ~ 50 kPa. Ground truth was recorded using a 50 fps video. Fig. 9 shows the results. The actuator exhibits approximately underdamped, second-order dynamics, with a damping ratio of ~ 0.03 and a damped natural frequency of ~ 2.8 Hz. This is comparable to the previously reported response times of 130 ms for similar actuators [14]. These oscillations are clearly visible in the sensor signal. However, there is additional slow creep in the sensor, which is

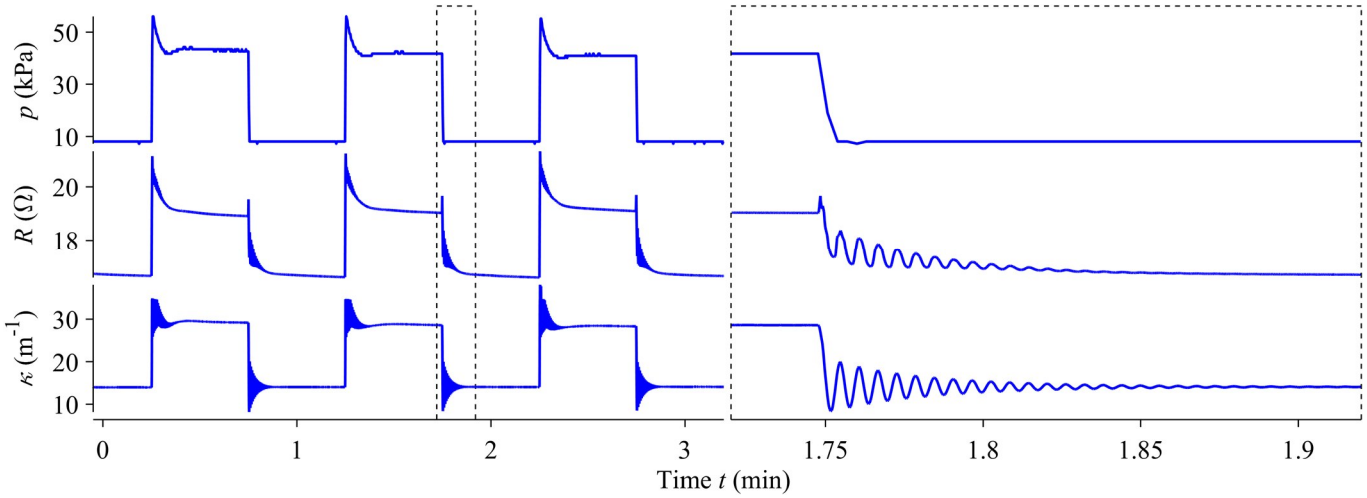

Fig. 9. Dynamics experiment. Several step experiments were done by fully opening or closing the valve. The actuator has approximately second-order dynamics and oscillates at around 2.8 Hz after a pressure step. The oscillations can easily be seen by the sensor, but there is additional slow creep in the sensor.

This work is licensed under a Creative Commons Attribution 3.0 License. For more information, see http://creativecommons.org/licenses/by/3.0/.

This article has been accepted for publication in a future issue of this journal, but has not been fully edited. Content may change prior to final publication. Citation information: DOI 10.1109/JSEN.2017.2765745, IEEE Sensors Journal

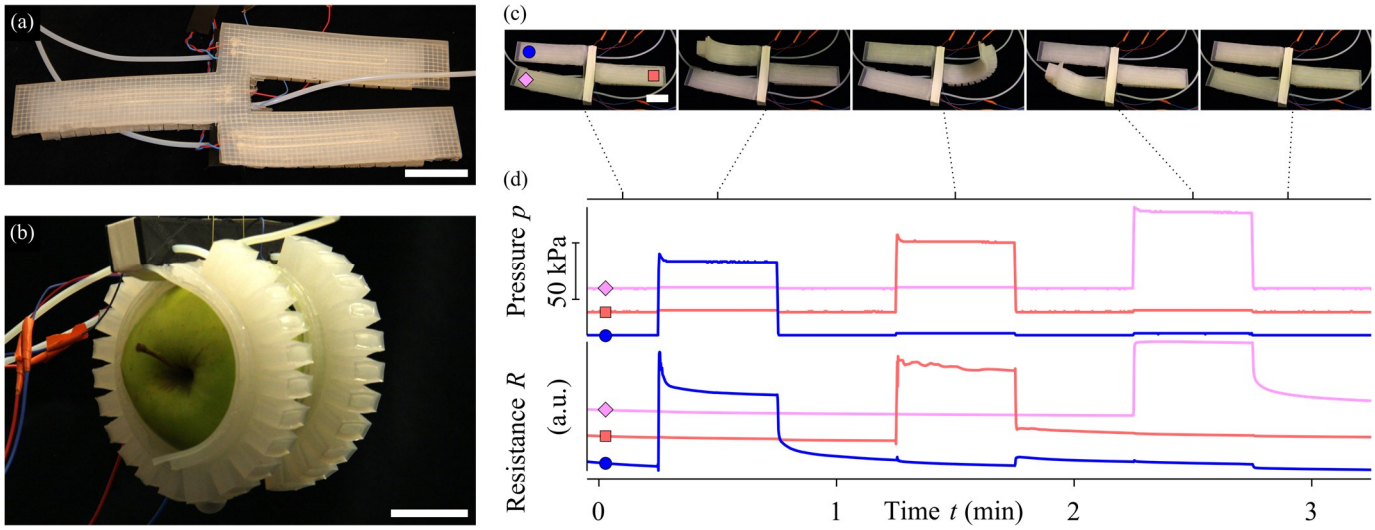

Fig. 10. Demonstration of the fabricated sensors in a soft robotic gripper. (a-b) A three-finger gripper in open and closed state. (c) Snapshots from the Supplementary Video, showing an experiment where all three fingers are actuated sequentially. (d) Pressure p and resistance R of the fingers during the experiment. Scale bars: 3 cm.

not seen in the ground truth. Such creep is typical for elastomer-based sensors and mathematical models have been developed to compensate for it.[40] We conclude that the dynamic response of the sensor is faster than that of the actuator, so the sensor is not limiting the sensor-actuator system bandwidth, but the slow creep limits the absolute accuracy of the sensor.

G. Integrating sensors into a three-fingered soft robotic gripper

To show a practical application of the smart actuators in soft robots, we fabricated a three-fingered gripper with sensors (Fig. 10). The fingers can be driven independently. One base was shared between the fingers and included the sensors. Fig. 10b shows the gripper picking up an object. Fig. 10c shows snapshots of an experiment where each of the fingers was sequentially actuated (see also the Supplementary Video for the experiment). Fig. 10d shows the resistances and pressures during the experiment. The channels are mostly independent. This demonstration shows that the sensors can be applied in practical robot designs.

IV. Conclusions

The screens and inks we used are readily available and the sensors can be printed directly onto elastomeric substrates in a timeframe of hours. Different sensor designs can be achieved simply by changing the screen stencil. The gauge factors, neutral resistances and dynamic characteristics vary from one sample to another, due to variations in the printing runs. We recommend calibrating every sensor individually. Also, the effects of hysteresis, temperature and creep limit the absolute accuracy of the sensors. We foresee using Preisach-type hysteresis models [41] to compensate for the hysteresis. Temperature effects could be reduced by using half-/full-bridge measurements. However, many practical robotic applications do not need absolute accuracy, only relative. For example, only relative measurement is needed to detect whether a soft robot finger has just collided with an object, as we have demonstrated.

Table I compares our results to the literature in which strain sensors have been applied for soft robotic actuators. In particular, Pinto *et al.* [29] have printed their carbon nanotube-based sensors with the aid of a stencil. Compared to that work, the main advantages of our method are: a) our sensors can be fabricated in a single print, instead of the two prints required in their method; b) using a mesh and a semi-automated screen-printer, the thickness can be controlled better than it can when the ink is applied manually through a stencil.

In Table I, we also see that the hysteresis values reported here are quite typical for resistive sensors. In particular, compared to [29], the hysteresis of our silver sensors was slightly lower. However, optical sensors generally have much lower hysteresis than resistive sensors, so they might be a better choice for applications where high-accuracy absolute measurements are needed. The main advantage of resistive sensing is the ease of measurement.

TABLE I
Comparison to Literature

Material /Product	Method[a]	Tested strains (%)	GF[b]	Hyste-resis (%)	Ref.
Silver ink	R	2	6	17	**This work**
Carbon ink	R	2	7	27	**This work**
Carbon nanotube ink	R	5	250 [c]	29 [d]	[29]
Gallium-Indium	R	23	2 [e]	5 [f]	[31]
Flex sensor®	R	< 10	7 [g]	13	[17]
Bend sensor®	R	< 10	40 [g]	10	[17]
Ionic hydrogels	C	490	0.7 [h]	-	[30]
Elastomer waveguide	O	100	-	~ 0	[33]
Polyethelene optical fiber	O	400	-	~ 0	[32]

[a] R = Resistive, C = Capacitive, O = Optical
[b] Gauge factor, $\Delta R/(R\varepsilon)$ for resistive sensors, $\Delta C/(C\varepsilon)$ for capacitive
[c] Estimated from Fig. 6a in [29] [d] Estimated from Fig. 9a in [29]
[e] Value from [42] [f] Estimated from Fig. 5 in [31]
[g] From Table 1 in [17] and using relation $\varepsilon = \theta r/L_0$, $L_0 = 50.8$ mm, $r = 10$ mm [h] Estimated from Fig. 2b in [30]

This work is licensed under a Creative Commons Attribution 3.0 License. For more information, see http://creativecommons.org/licenses/by/3.0/.

This article has been accepted for publication in a future issue of this journal, but has not been fully edited. Content may change prior to final publication. Citation information: DOI 10.1109/JSEN.2017.2765745, IEEE Sensors Journal

Finally, Table I shows that the strains we tested are quite low compared to other studies. This is not due to a fundamental limitation of our sensor, but a consequence of the sensor placement in our actuators. Our coauthors have previously shown that the silver ink does not fail, even at 50 % strains. [37] In summary, we have shown that screen-printing is a promising route for the integration of curvature sensors into soft robots. This clears the path towards soft robots that react to their surroundings.

ACKNOWLEDGEMENT

A.K. and E.S.R. contributed equally to the work. V.S. and M. Mäntysalo conceived the research. E.S.R. built the characterization setup. A.K. performed the characterization experiments. A.K. and E.S.R. fabricated the actuators. V.S. analyzed the results. M. Mosallaei fabricated the sensors. A.K., E.S.R. and V.S. wrote the paper with inputs from all authors. We thank Timo Aho for the scanning electron micrograph, and Sampo Tuukkanen, Ville Liimatainen and Pasi Kallio for insightful comments on the draft of this manuscript.

REFERENCES

[1] D. Trivedi, C. D. Rahn, W. M. Kier, and I. D. Walker, "Soft robotics: Biological inspiration, state of the art, and future research," *Appl. Bionics Biomech.*, vol. 5, no. 3, pp. 99–117, 2008.

[2] F. Ilievski, A. D. Mazzeo, R. F. Shepherd, X. Chen, and G. M. Whitesides, "Soft robotics for chemists," *Angew. Chemie - Int. Ed.*, vol. 50, no. 8, pp. 1890–1895, 2011.

[3] C. Majidi, "Soft Robotics: A Perspective—Current Trends and Prospects for the Future," *Soft Robot.*, vol. 1, no. 1, pp. 5–11, 2014.

[4] D. Rus and M. T. Tolley, "Design, fabrication and control of soft robots," *Nature*, vol. 521, no. 7553, pp. 467–475, 2015.

[5] E. Brown, N. Rodenberg, J. Amend, A. Mozeika, E. Steltz, M. R. Zakin, H. Lipson, and H. M. Jaeger, "Universal robotic gripper based on the jamming of granular material," *Proc. Natl. Acad. Sci.*, vol. 107, no. 44, pp. 18809–18814, 2010.

[6] S. Song and M. Sitti, "Soft grippers using micro-fibrillar adhesives for transfer printing," *Adv. Mater.*, vol. 26, no. 28, pp. 4901–4906, 2014.

[7] R. Deimel and O. Brock, "A novel type of compliant and underactuated robotic hand for dexterous grasping," *Int. J. Rob. Res.*, vol. 35, no. 1–3, pp. 161–185, 2016.

[8] K. Suzumori, S. Endo, T. Kanda, N. Kato, and H. Suzuki, "A bending pneumatic rubber actuator realizing soft-bodied manta swimming robot," *Proc. IEEE Int. Conf. Robot. Autom.*, no. April, pp. 4975–4980, 2007.

[9] S.-J. Park, M. Gazzola, K. S. Park, S. Park, V. Di Santo, E. L. Blevins, J. U. Lind, P. H. Campbell, S. Dauth, A. K. Capulli, F. S. Pasqualini, S. Ahn, A. Cho, H. Yuan, B. M. Maoz, R. Vijaykumar, J.-W. Choi, K. Deisseroth, G. V. Lauder, L. Mahadevan, and K. K. Parker, "Phototactic guidance of a tissue-engineered soft-robotic ray," *Science*, vol. 353, no. 6295, pp. 158–162, 2016.

[10] R. F. Shepherd, F. Ilievski, W. Choi, S. Morin, A. Stokes, A. Mazzeo, X. Chen, M. Wang, and G. Whitesides, "Multigait soft robot," *Proc. Natl. Acad. Sci.*, vol. 108, no. 51, pp. 20400–20403, 2011.

[11] P. Polygerinos, Z. Wang, K. C. Galloway, R. J. Wood, and C. J. Walsh, "Soft robotic glove for combined assistance and at-home rehabilitation," *Rob. Auton. Syst.*, vol. 73, pp. 135–143, 2015.

[12] Y. Menguc, Y.-L. Park, H. Pei, D. Vogt, P. M. Aubin, E. Winchell, L. Fluke, L. Stirling, R. J. Wood, and C. J. Walsh, "Wearable soft sensing suit for human gait measurement," *Intenational J. Robot. Res.*, vol. 33, no. 14, pp. 1748–1764, 2014.

[13] Keiko Ogura, S. Wakimoto, K. Suzumori, and Yasutaka Nishioka, "Micro pneumatic curling actuator - Nematode actuator," in *Proceedings IEEE International Conference on Robotics and Biomimetics*, 2008, pp. 462–467.

[14] B. Mosadegh, P. Polygerinos, C. Keplinger, S. Wennstedt, R. F. Shepherd, U. Gupta, J. Shim, K. Bertoldi, C. J. Walsh, and G. M. Whitesides, "Pneumatic networks for soft robotics that actuate rapidly," *Adv. Funct. Mater.*, vol. 24, no. 15, pp. 2163–2170, 2014.

[15] R. K. Katzschmann, A. D. Marchese, and D. Rus, "Hydraulic autonomous soft robotic fish for 3D swimming," *Springer Tracts Adv. Robot.*, vol. 109, no. 1122374, pp. 405–420, 2016.

[16] D. P. Holland, E. J. Park, P. Polygerinos, G. J. Bennett, and C. J. Walsh, "The Soft Robotics Toolkit : Shared Resources for Research and Design," vol. 1, no. 3, pp. 224–230, 2014.

[17] D. H. Kim, S. W. Lee, and H. S. Park, "Sensor evaluation for soft robotic hand rehabilitation devices," in *Proc. IEEE RAS EMBS Int. Conf. Biomed. Robot. Biomech.*, 2016, pp. 1220–1223.

[18] G. Gerboni, A. Diodato, G. Ciuti, M. Cianchetti, and A. Menciassi, "Feedback control of soft robot actuators via commercial flex bend sensors," *IEEE/ASME Trans. Mechatronics*, vol. 4435, no. c, pp. 1–1, 2017.

[19] S. Ozel, N. A. Keskin, D. Khea, and C. D. Onal, "A precise embedded curvature sensor module for soft-bodied robots," *Sensors Actuators, A Phys.*, vol. 236, pp. 349–356, 2015.

[20] M. Amjadi, K. U. Kyung, I. Park, and M. Sitti, "Stretchable, Skin-Mountable, and Wearable Strain Sensors and Their Potential Applications: A Review," *Adv. Funct. Mater.*, vol. 26, no. 11, pp. 1678–1698, 2016.

[21] Kenry, J. C. Yeo, and C. T. Lim, "Emerging flexible and wearable physical sensing platforms for healthcare and biomedical applications," *Microsystems Nanoeng.*, vol. 2, no. April, p. 16043, 2016.

[22] H. Nakamoto, H. Ootaka, M. Tada, I. Hirata, F. Kobayashi, and F. Kojima, "Stretchable Strain Sensor with Anisotropy and Application for Joint Angle Measurement," *IEEE Sens. J.*, vol. 16, no. 10, pp. 3572–3579, 2016.

[23] H. Nakamoto, H. Ootaka, M. Tada, I. Hirata, F. Kobayashi, and F. Kojima, "Stretchable strain sensor based on areal change of carbon nanotube electrode," *IEEE Sens. J.*, vol. 15, no. 4, pp. 2212–2218, 2015.

[24] J. Shi, X. Li, H. Cheng, Z. Liu, L. Zhao, T. Yang, Z. Dai, Z. Cheng, E. Shi, L. Yang, Z. Zhang, A. Cao, H. Zhu, and Y. Fang, "Graphene Reinforced Carbon Nanotube Networks for Wearable Strain Sensors," *Adv. Funct. Mater.*, vol. 26, no. 13, pp. 2078–2084, 2016.

[25] C. Mattmann, F. Clemens, and G. Tröster, "Sensor for measuring strain in textile," *Sensors*, vol. 8, no. 6, pp. 3719–3732, 2008.

[26] E. L. White, J. C. Case, and R. K. Kramer, "Multi-mode strain and curvature sensors for soft robotic applications," *Sensors Actuators, A Phys.*, vol. 253, pp. 188–197, 2017.

[27] M. Amjadi, A. Pichitpajongkit, S. Lee, S. Ryu, and I. Park, "Highly Stretchable and Sensitive Strain Sensor Based on Silver-Elastomer Nanocomposite," *ACS Nano*, vol. 8, no. 5, pp. 5154–5163, 2014.

[28] F. Xu and Y. Zhu, "Highly conductive and stretchable silver nanowire conductors," *Adv. Mater.*, vol. 24, no. 37, pp. 5117–5122, 2012.

[29] T. Pinto, L. Cai, C. Wang, and X. Tan, "CNT-based sensor arrays for local strain measurements in soft pneumatic actuators," *Int. J. Intell. Robot. Appl.*, vol. 1, no. 2, pp. 157–166, 2017.

[30] C. Larson, B. Peele, S. Li, S. Robinson, M. Totaro, L. Beccai, B. Mazzolai, and R. Shepherd, "Highly Stretchable Electroluminescent Skin for Optical Signaling and Tactile Sensing," *Science*, vol. 351, no. 6277, pp. 1071–1074, 2016.

[31] Y. L. Park and R. J. Wood, "Smart pneumatic artificial muscle actuator with embedded microfluidic sensing," in *Proc. IEEE Sensors*, 2013.

[32] S. Sareh, Y. Noh, M. Li, T. Ranzani, H. Liu, and K. Althoefer, "Macrobend optical sensing for pose measurement in soft robot arms," *Smart Mater. Struct.*, vol. 24, no. 12, p. 125024, 2015.

[33] H. Zhao, K. O 'brien, S. Li, and R. F. Shepherd, "Optoelectronically innervated soft prosthetic hand via stretchable optical waveguides," *Sci. Robot.*, vol. 7529, no. 1, p. eaai7529, 2016.

[34] C. M. Homenick, R. James, G. P. Lopinski, J. Dunford, J. Sun, H. Park, Y. Jung, G. Cho, and P. R. L. Malenfant, "Fully Printed and Encapsulated SWCNT-Based Thin Film Transistors via a Combination of R2R Gravure and Inkjet Printing," *ACS Appl. Mater. Interfaces*, vol. 8, no. 41, pp. 27900–27910, 2016.

This work is licensed under a Creative Commons Attribution 3.0 License. For more information, see http://creativecommons.org/licenses/by/3.0/.

This article has been accepted for publication in a future issue of this journal, but has not been fully edited. Content may change prior to final publication. Citation information: DOI 10.1109/JSEN.2017.2765745, IEEE Sensors Journal

[35] T. Vuorinen, J. Niittynen, T. Kankkunen, T. M. Kraft, and M. Mäntysalo, "Inkjet-Printed Graphene/PEDOT:PSS Temperature Sensors on a Skin-Conformable Polyurethane Substrate," *Sci. Rep.*, vol. 6, no. 1, p. 35289, 2016.

[36] S. L. Swisher, M. C. Lin, A. Liao, E. J. Leeflang, Y. Khan, F. J. Pavinatto, K. Mann, A. Naujokas, D. Young, S. Roy, M. R. Harrison, A. C. Arias, V. Subramanian, and M. M. Maharbiz, "Impedance sensing device enables early detection of pressure ulcers in vivo," *Nat. Commun.*, vol. 6, p. 6575, 2015.

[37] J. Suikkola, T. Björninen, M. Mosallaei, T. Kankkunen, P. Iso-Ketola, L. Ukkonen, J. Vanhala, and M. Mäntysalo, "Screen-Printing Fabrication and Characterization of Stretchable Electronics.," *Sci. Rep.*, vol. 6, no. April, p. 25784, 2016.

[38] R. J. Webster and B. A. Jones, "Design and Kinematic Modeling of Constant Curvature Continuum Robots: A Review," *Int. J. Rob. Res.*, vol. 29, no. 13, pp. 1661–1683, 2010.

[39] S. Merilampi, T. Björninen, V. Haukka, P. Ruuskanen, L. Ukkonen, and L. Sydänheimo, "Analysis of electrically conductive silver ink on stretchable substrates under tensile load," *Microelectron. Reliab.*, vol. 50, no. 12, pp. 2001–2011, 2010.

[40] K. Le Phan, "Methods to correct for creep in elastomer-based sensors," in *2008 IEEE Sensors*, 2008, pp. 1119–1122.

[41] I. Mayergoyz, "Mathematical models of hysteresis," *IEEE Trans. Magn.*, vol. 22, no. 5, pp. 603–608, Sep. 1986.

[42] C. Majidi, R. Kramer, and R. J. Wood, "A non-differential elastomer curvature sensor for softer-than-skin electronics," *Smart Mater. Struct. Smart Mater. Struct*, vol. 20, no. 20, pp. 105017–7, 2011.

Anastasia Koivikko received her B.Sc. and M.Sc. degrees in biomedical engineering from Tampere University of Technology, Tampere, Finland, in 2015 and 2017, respectively. Currently, she is pursuing a Ph.D. degree in the same university. Her research interests include fabrication of soft robots.

Ehsan Sadeghian Raei received a B.Sc. degree in biomedical engineering from Azad University, Mashhad, Iran, in 2011 and an M.Sc. degree in electrical engineering from Tampere University of Technology, Tampere, Finland, in 2016. He is currently pursuing a Ph.D. degree in biomedical engineering at Tampere University of Technology, Tampere, Finland. His research interests include energy-harvesting, thermoelectric materials, pneumatic actuators and sensors for biomedical soft robots.

Mahmoud Mosallaei received a B.Sc. degree in Polymer Industries Engineering from Shiraz Azad University, Shiraz, Iran, in 2007 and an M.Sc. degree in Materials Science from Tampere University of Technology (TUT), Tampere, Finland, in 2015. He is currently pursuing a Doctoral degree in Computing and Electrical Engineering at TUT. He finished his master's thesis with IMEC, Leuven, Belgium in 2015. His research interests are mainly printed electronics, soft and deformable materials toward the development of stretchable electronic devices.

Matti Mäntysalo (M'09) received his M.Sc. and D.Sc. (Tech) degrees in electrical engineering in Tampere University of Technology, Tampere, Finland in 2004 and 2008, respectively.

He is an Associate Professor of Electronics Materials and Manufacturing and an Academy of Finland Research fellow. He has been awarded the title of Adjunct Professor in Digital fabrication.

His research interests include printed electronics materials, fabrication processes, stretchable and soft electronics, and especially the integration of printed electronics with silicon-based technology (hybrid systems). He has authored or co-authored more than 100 international journal and conference articles. Mäntysalo has been active in IEEE CMPT, IEC TC119 Printed electronics standardization, and Organic Electronics Association.

Veikko Sariola (M'17) is an Assistant Professor in Bio-MEMS at the Tampere University of Technology, in Finland. In 2012, he obtained his Dr. Tech. degree in Electrical Engineering from Aalto University, Finland.

From 2013 to 2015, he was a post-doctoral researcher at Carnegie Mellon University, and in 2016, he was appointed as a Research Fellow of the Academy of Finland. His current research interests include bio-inspired materials and robotics.

This work is licensed under a Creative Commons Attribution 3.0 License. For more information, see http://creativecommons.org/licenses/by/3.0/.